Asian Journal of Civil Engineering
https://doi.org/10.1007/s42107-023-00924-7

RESEARCH

Predicting shear capacity of rectangular hollow RC columns using neural networks

Xuan-Bang Nguyen[1] · Viet-Linh Tran[2] · Huy-Thien Phan[2] · Duy-Duan Nguyen[2]

Received: 18 October 2023 / Accepted: 24 October 2023

Abstract
This study predicts the shear strength of rectangular hollow reinforced concrete (RC) columns using artificial neural network (ANN). A total of 120 experimental results are collected from literature and used for establishing the machine learning model. The results reveal that the proposed ANN model predicts the shear strength of rectangular hollow RC columns accurately with R^2 of 0.99. Additionally, the relative importance of input parameters on the calculated shear strength of RC columns is evaluated using Shapley value. Based on the ANN model, a graphical user interface tool is also developed and readily used in predicting the shear strength of rectangular hollow RC columns.

Keywords Rectangular hollow reinforced concrete column · Shear strength · Artificial neural network · Graphical user interface

Introduction

Rectangular hollow reinforced concrete (RC) columns have been widely used in bridge structures, since they satisfy both the efficiently lateral loading capacity and beneficial construction costs (Cassese et al., 2020; Kim et al., 2014a, 2014b; Mo et al., 2001; Pinto et al., 2003; Sun et al., 2019; Yang et al., 2019; Yeh et al., 2002a, 2002b). Understanding of failure modes is the crucial issue for designing new structures, retrofitting the existing ones properly. Numerous experimental studies reported that the RC column can be failed in flexure, shear, or flexure–shear, depending on geometric dimensions, reinforcing bar details, and material properties.

Several conventional approaches were employed to identify the failure modes of RC columns with solid cross-sections. Simply, failure types of rectangular RC columns can be predicted using the aspect ratio, a/d (i.e., shear span-to-effective depth ratio). If $a/d \geq 4$, the column fails in flexure; if $2 < a/d < 4$, a flexure–shear failure is governed; if $a/d \leq 2$, the shear failure is dominated (Qi et al., 2013). However, the effects of material properties and reinforcement details were not reflected in this approach (Feng et al., 2020). Another indicator, the shear strength ratio (V_r), i.e., the ratio of the shear demand to shear capacity, can be used for predicting the failure modes of rectangular RC columns (Pekelnicky et al., 2012; Qi et al., 2013). The column suffers shear failure if $V_r > 1$, the column fails in flexure if $V_r \leq 0.6$, and otherwise, a flexure–shear failure is dominated. However, it was also pointed out that this method owned a deficiency and, therefore, predicted failure modes of solid RC columns less accurately (Ma & Gong, 2018; Qi et al., 2013; Zhu et al., 2007). Furthermore, Ghee et al. (1989) used the displacement ductility factor, μ (i.e., the ratio of the displacement at the maximum shear strength to the yield displacement), to classify failure modes of circular RC columns. If $\mu \geq 6$, the column fails in flexure; a ductile–shear failure can be exhibited if $2 < \mu < 6$; and otherwise, if $\mu \leq 2$, a shear failure is governed. Nevertheless, they conducted a small set of experiments thus, it was insufficient to apply for a wide range of columns.

✉ Duy-Duan Nguyen
duyduankxd@vinhuni.edu.vn

Xuan-Bang Nguyen
nxb@lqdtu.edu.vn

Viet-Linh Tran
vietlinhkxd@vinhuni.edu.vn

Huy-Thien Phan
huythienkxd@vinhuni.edu.vn

[1] Institute of Techniques for Special Engineering, Le Quy Don Technical University, Hanoi, Vietnam

[2] Department of Civil Engineering, Vinh University, Vinh 461010, Vietnam

Published online: 02 December 2023

Machine learning (ML) techniques have been extensively applied in various engineering problems since it owns great advantages such as computational efficiency and sufficient consideration of uncertainties (Falcone et al., 2020; Kaveh & Khavaninzadeh, 2023). Numerous studies used ML techniques to estimate the structural response of civil structures (Caglar et al., 2009; Farfani et al., 2015; Gharehbaghi et al., 2019; Morfidis & Kostinakis, 2018; Razzaghi et al., 2018). The mentioned studies highlighted the capability of used ML techniques in estimating responses and failure modes of structures, and some methods showed to be superior compared with others. Artificial neural network (ANN) is one of the most efficient ML models in predicting structural responses of RC structures (Asteris & Mokos, 2019; Kaveh et al., 2021, 2023; Mai et al., 2022; Nguyen et al., 2021a, 2021b; Tran et al., 2020, 2022).

Recently, several studies have applied ML techniques to predict the shear capacity of RC columns with solid sections, in which typical works are Mangalathu and Jeon (2019), Feng et al. (2020), Mangalathu et al. (2020), and Phan et al. (2022). They highlighted the excellent performance of ML in prediction problems. However, there are no ML studies on predicting shear strength of hollow RC columns so far.

Empirical formulas in previous studies and design codes are mostly focused on calculation of the shear strength of solid RC columns (ACI-318–14, 2014; ASCE/SEI-41-06, 2007; Ascheim & Moehle, 1992; Biskinis et al., 2004; Cassese et al., 2019; EN-, 1998–1, 2004; Kowalsky & Priestley, 2000; Priestley et al., 1994; Sezen & Moehle, 2004). Those expressions have been widely applied for hollow RC columns. However, a large scatter is still existing in comparison between experimental tests and predictive equations, even though a specific model (Shin et al., 2013) is proposed for calculating the shear strength of hollow RC columns.

This study applies ANN model, which is developed based on 120 experimental data, to predict the shear strength of rectangular RC columns with hollow cross-section types. The result of ANN is then compared with that of predicted by seven published empirical formulas. Additionally, the relative importance of input parameters on the calculated shear strength of RC columns is evaluated using Shapley value. Moreover, a graphical user interface (GUI) tool, which can be readily used in the design process and structural performance evaluation, is developed for predicting the shear strength of rectangular hollow RC columns.

Description of experimental data

To develop ML techniques, a set of 120 experimental test results of RC columns with the rectangular hollow cross-section was collected from the literature (Calvi et al., 2005; Cheng et al., 2005; Faria et al., 2004; Han et al., 2013; Kim, 2019; Kim et al., 2019; Mo & Nien, 2002; Mo et al., 2003; Pinto et al., 2003; Shin et al., 2013; Yang et al., 2019; Yeh et al., 2002a). Eleven input parameters, including geometric dimensions, reinforcing bar details, material properties, and axial load, need to be provided to estimate the shear strength of RC columns. Geometric dimensions comprise of the height of the column (L_v), the width of the cross-section (B), the length of the cross-section (H), and the wall thickness (t_w). Reinforcement details include the longitudinal reinforcement ratio (ρ_l), the transversal reinforcing bar ratio (ρ_w), and the spacing of the transversal reinforcements (s). Material properties are the yield strength of the longitudinal (f_{yl}) and transversal (f_{yw}) reinforcing bars and the compressive strength of concrete ($f_c{'}$). The axial load (P) is also considered in the database.

Figure 1 schematically shows the configurations and reinforcement properties of the rectangular hollow RC column. The statistical properties of the experimental results are described in Table 1. In this table, eleven input parameters are numbered as variables from X1 to X11 to

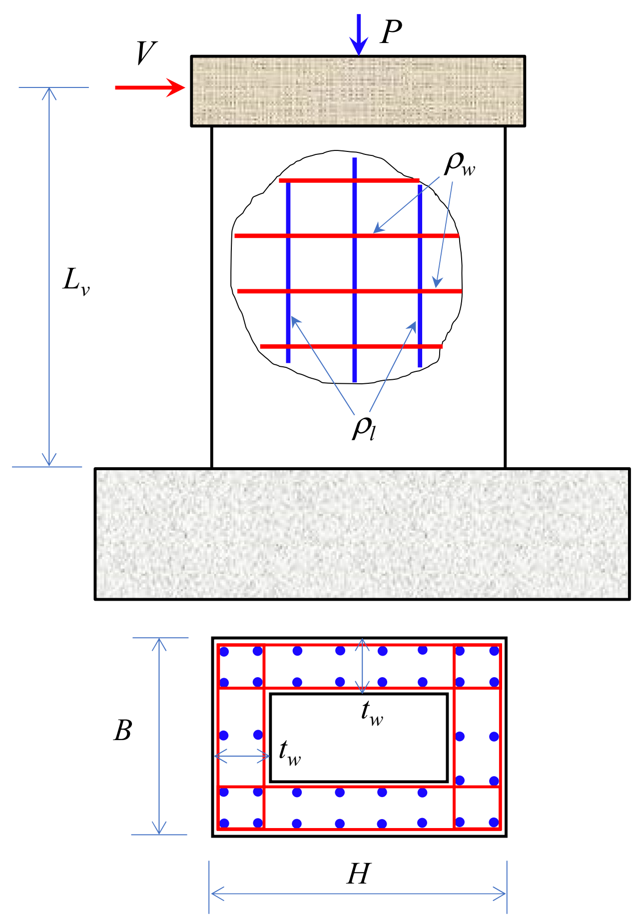

Fig. 1 Configurations and properties of rectangular hollow RC columns

Table 1 Statistical properties of input parameters of used database

Input parameter	L_v (mm)	B(mm)	H(mm)	t_w (mm)	ρ_l (%)	ρ_w (%)	s (mm)	f_c' (MPa)	f_{yl} (MPa)	f_{yw} (MPa)	P(kN)
(Variable)	(X1)	(X2)	(X3)	(X4)	(X5)	(X6)	(X7)	(X8)	(X9)	(X10)	(X11)
Min	650	320	250	70	0.19	0.0	30	17	270	235	0.0
Mean	2455	626.7	725.7	139.7	1.65	0.18	191.20	35.7	411.9	398.4	1250.6
Max	13,250	1500	2740	300	6.41	1.60	1800	70	625	700	8799.8
SD	1740.8	309.6	426.2	62.7	0.84	0.22	354.5	11.9	97.8	101.7	1394.9
COV	0.71	0.49	0.59	0.45	0.51	1.22	1.85	0.33	0.24	0.26	1.12

consider in performing machine learning models. The frequency histograms of input parameters and failure modes of the 120 collected data are shown in Fig. 2. For this database, the number of columns failed in flexure (F), flexure–shear combination (FS), and shear (S) is 60, 42, and 18, respectively.

Overview of ANN model

In addition to aforesaid classification techniques, the ANN model was used for predicting the shear strength of rectangular hollow RC columns. An ANN model comprises

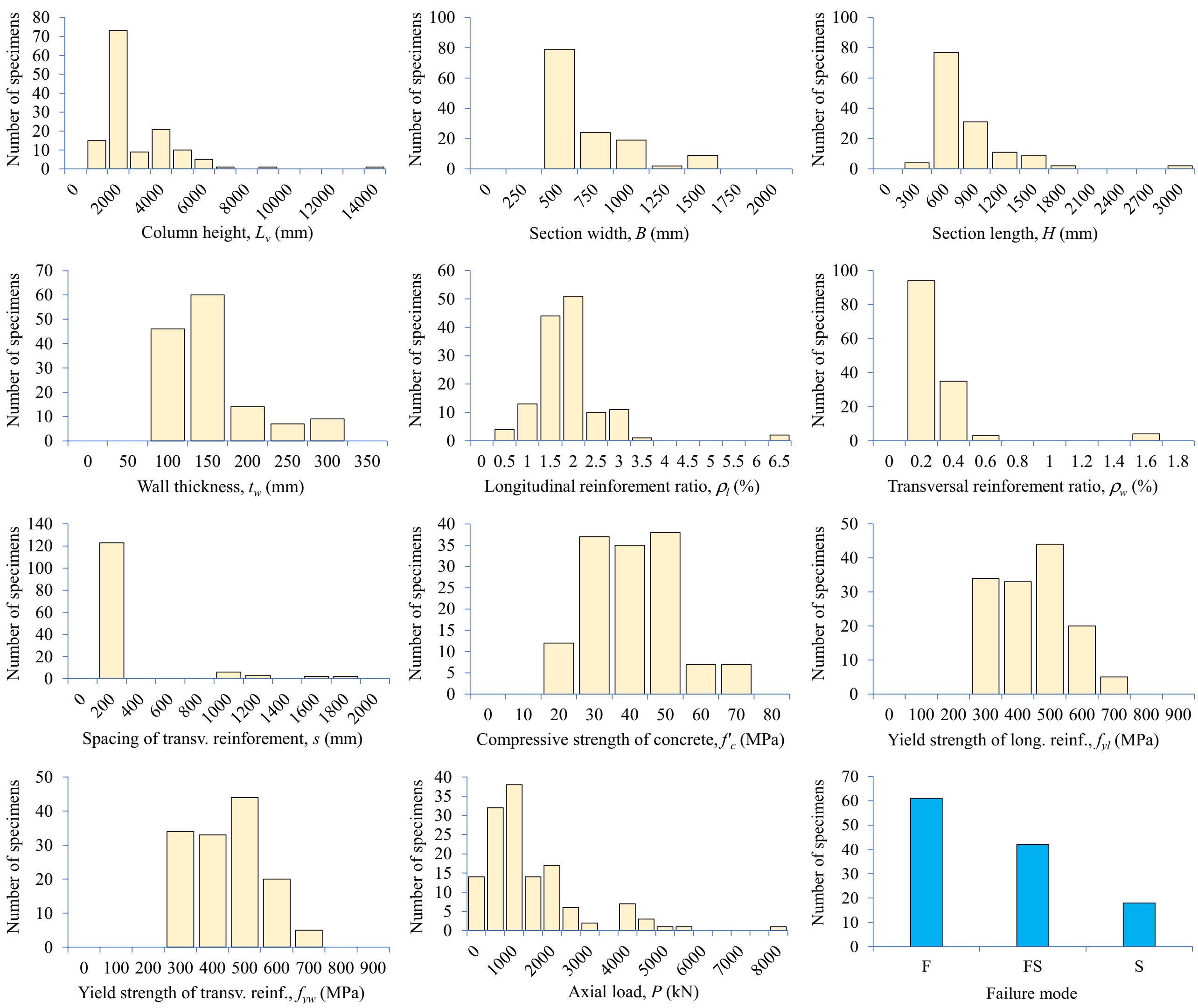

Fig. 2 Histograms of input parameters and observed failure modes of experimental data

of three components:

(1) Input layer, where input parameters are entered,
(2) Hidden layer(s), and
(3) Output layer, where the predicted result is obtained.

In this study, the tansig and purelin functions were employed for hidden and output layer, respectively. These functions aim to make a transition during training the network smoothly, expressed by Eqs. (1) and (2).

$$y = \text{tansig}(x) = \frac{2}{1 + e^{-2x}} - 1 \tag{1}$$

$$y = \text{purelin}(x) = x. \tag{2}$$

To perform the ANN algorithm, following processes are required:

(1) Firstly, the input data are provided to the input layer, the signals are transferred through the connections, from one node (i.e., neuron) to another in the network. This is called the forward pass.
(2) Secondly, after obtaining the output from the forward pass, it is required to evaluate this output by comparing it with the target using the mean squared error (MSE), as expressed in Eq. (3). This is called the backward pass.
(3) Moreover, it is needed to minimize the error by iteratively updating those processes until *MSE* is converged.

$$\text{MSE} = \frac{1}{N}\sum_{i=1}^{N}\left(p_i - t_i\right)^2, \tag{3}$$

where N is the number of samples; t_i and p_i are the target and predicted values of the ith sample, respectively. Figure 3 shows the structure of the ANN model, in which the input layer contains eleven parameters, the hidden layer includes eight neurons, and the output layer is the predicted shear strength.

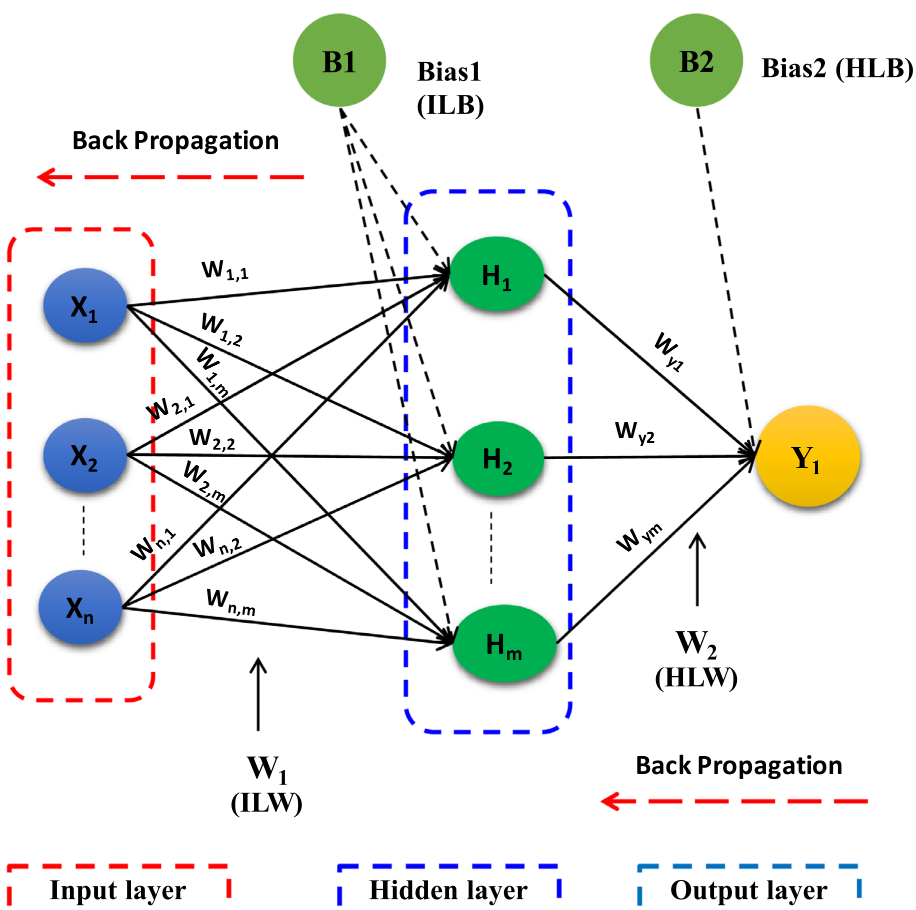

Fig. 3 Depiction of ANN structure

Table 2 Equations for calculating the shear strength of rectangular hollow RC columns

No	Reference	Equation	
1	Ascheim and Moehle (1992)	$V_{R1} = V_{\mathrm{c}} + V_{\mathrm{w}}$ $V_{\mathrm{c}} = 0.3\left(k + \frac{P}{13.8A_{\mathrm{g}}}\right)0.8A_g\sqrt{f_{\mathrm{c}}\prime}$ $k = \frac{4-\mu}{3}$, μ is the displacement ductility $V_w = \frac{A_{sw}f_{yw}d}{s\tan(30^0)}; d = 0.8H$	(4)
2	Priestley et al. (1994)	$V_{R2} = V_c + V_w + V_p$ $V_c = 0.8A_g k\sqrt{f_c'}$ $k = 0.29$ for $\mu < 2$ $k = 0.29 - 0.12(\mu - 2)$ for $2 < \mu < 4$ $k = 0.10$ for $\mu > 4$ $V_{\mathrm{w}} = \frac{A_{\mathrm{sw}}f_{\mathrm{yw}}D\prime}{s}\cot(30^0)$ $V_{\mathrm{p}} = P\tan(\alpha) = \frac{D-c}{2a}P$	(5)
3	Kowalsky and Priestley (2000)	$V_{R3} = V_c + V_w$ $V_{\mathrm{c}} = \alpha\beta k 0.8A_g\sqrt{f_c'}$ $1 \le \alpha = 3 - \frac{L_{\mathrm{v}}}{H} \le 1.5;$ $\beta = 0.5 + 20\rho_l \le 1$ $k = 0.29$ for $\mu < 2.0$ $k = 0.05$ for $\mu > 8.0$ $V_{\mathrm{w}} = \frac{A_{\mathrm{sw}}f_{\mathrm{yw}}(D\prime - c)}{s}\cot(30^0)$	(6)
4	Sezen and Moehle (2004)	$V_{\mathrm{R4}} = V_c + V_s$ $V_{\mathrm{c}} = k\left(\frac{0.5\sqrt{f_{\mathrm{c}}\prime}}{a/d}\sqrt{1 + \frac{P}{0.5A_g\sqrt{f_c'}}}\right)0.8A_{\mathrm{g}}$; $d = D -$ cover $V_{\mathrm{s}} = k\frac{A_{\mathrm{sw}}f_{\mathrm{yw}}d}{s}$ $k = 1$ for $\mu < 2.0$ $k = 0.7$ for $\mu > 6.0$ a is the shear span, i.e., the distance from loading point to the boundary	(7)
5	Biskinis et al. (2004)	$V_{\mathrm{R5}} = V_{\mathrm{p}} + k(V_{\mathrm{c}} + V_{\mathrm{w}})$ $V_{\mathrm{c}} = 0.16\max(0.5;100\rho_l)\left(1 - 0.16\min\left(5;\frac{a}{d}\right)\right)A_{\mathrm{c}}\sqrt{f_{\mathrm{c}}\prime}$ $V_{\mathrm{w}} = \frac{A_{\mathrm{sw}}}{s}(d - d\prime)f_{\mathrm{yw}}$ $V_{\mathrm{p}} = \frac{D-x}{2a}\min(P;0.55A_{\mathrm{c}}f_{\mathrm{c}}\prime)$ x is the neutral axis depth, $d\prime$ is the depth of the compression reinforcement layer $k = 1 \sim 0.75$ for $\mu < 1 \sim 6$ $A_{\mathrm{c}} = b_{\mathrm{w}}d$, ($d = 0.8H$ is the effective depth);	(8)
6	Shin et al. (2013)	$V_{R6} = (\alpha\beta k)5\sqrt{f_{\mathrm{c}}\prime}\sqrt{1 + \frac{P}{0.5A_{\mathrm{g}}\sqrt{f_{\mathrm{c}}\prime}}}\left(A_{\mathrm{e}}\right) + \frac{A_{\mathrm{v}}f_{\mathrm{vy}}d}{s}; d = 0.8H;$ $\alpha = 1.35 - 0.3\frac{L_v}{H}(1.5 \le \frac{L_v}{H} \le 3);$ $\beta = 0.5 + 20\rho_l \le 1;$ $\gamma = \frac{8-\mu}{6}(2 \le \mu \le 5;$	(9)
7	Cassese et al. (2019)	$V_{\mathrm{R7}} = \alpha\beta k\sqrt{f_{\mathrm{c}}\prime}\left(2t_{\mathrm{w}}d\right); d = 0.8H;$ $1 \le \alpha = 3 - \frac{L_{\mathrm{v}}}{H} \le 1.5;$ $\beta = 0.5 + 20\rho\prime \le 1$; $\rho\prime = \frac{A}{BH}$	(10)

Results and discussion

Previous studies mostly proposed equations for calculating the shear strength of solid RC columns (ACI-318-14, 2014; ASCE/SEI-41-06, 2007; Ascheim & Moehle, 1992; Biskinis et al., 2004; Cassese et al., 2019; EN-, 1998–1, 2004; Kowalsky & Priestley, 2000; Priestley et al., 1994; Sezen & Moehle, 2004). Those equations also have been applied for hollow RC columns. However, the hollow columns may expose a different behavior from the solid ones subjected to lateral loads (Cassese, 2017; Shin et al., 2013). So far, only one specific equation for predicting

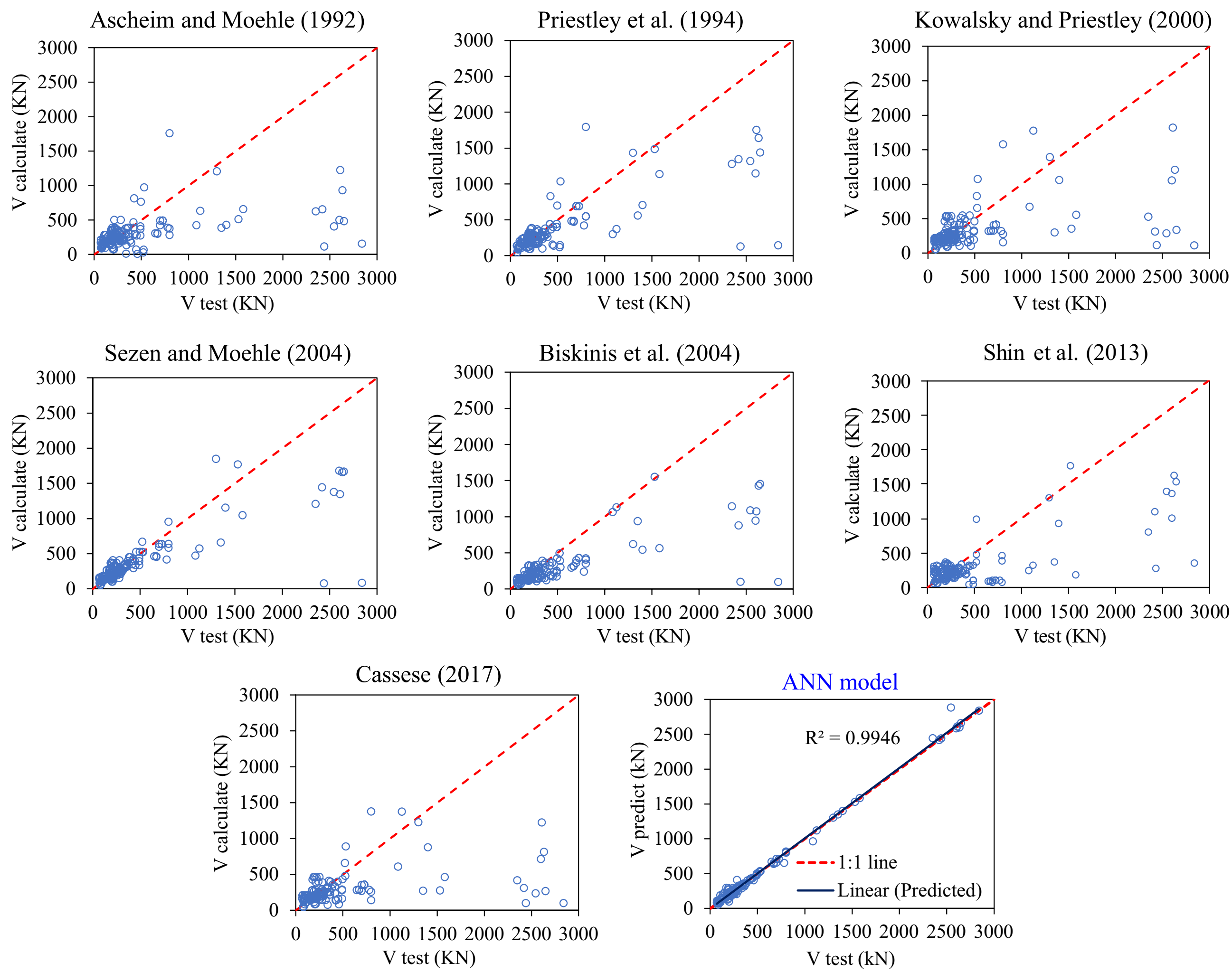

Fig. 4 Comparison of shear strength between experiments and various calculated models

Fig. 5 Relative importance of each feature

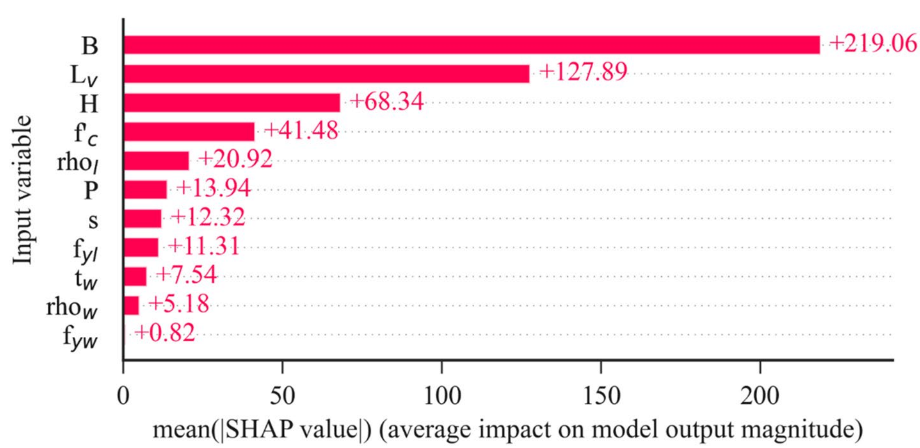

shear strength of hollow RC columns was developed by Shin et al. (Shin et al., 2013). In this study, we employed seven typical equations for estimating the shear strength of the hollow RC columns, as expressed in Table 2.

The comparisons of predictive models and experimental results are presented in Fig. 4. It was obviously demonstrated that the result of the ANN model has a smallest scattering with R^2 of 0.995, while existing models contain a wider deviation from the 1:1 line. This observation highlighted that the ANN model can be the optimal model for calculating the shear strength of rectangular hollow RC columns. The second best option was the model of Sezen and Moehle (2004), even though some discrepancies between calculated and experimental results were existing.

To explore how the predictions of the shear stregnth are affected by the input variables in the ANN model, the SHAP method is also adopted. The importance of the input variables in predicting the shear strength of hollow RC columns is presented in Fig. 5. These figures show that the most influential feature to the shear strength is B, followed by the L_v, H, $f_c\prime$, ρ_l, P, s, f_{yl}, t_w, ρ_w, and f_{yw}. It is also observed that ρ_l, P, s, f_{yl}, t_w, ρ_w, and f_{yw} slightly impact the ANN model's outputs.

To apply proposed ML models in specific problems, a convenient tool needs to be established. We developed a Graphical User Interface (GUI) in MATLAB for facilitating failure modes identification as well as prediction of the shear strength of rectangular hollow RC columns, as shown in Fig. 6. Eleven input parameters need to be provided. The failure modes and the shear strength of the column are readily obtained after filling the required inputs. It takes a few seconds to achieve the predictive results. It should be noted that the GUI tool is provided freely at https://github.com/duyduan1304/GUI_RCHollowColumn.

Conclusions

The failure modes of rectangular hollow RC columns were identified using six novel machine learning (ML) techniques, which were established based on 120 experimental results. Six ML models included Naïve Bayes (NB), K-nearest Neighbors (KNN), Decision Tree (DT), and Support Vector Machine (SVM) with Linear, Gaussian, and Polynomial kernel functions. Meanwhile, the Artificial Neural Network (ANN) technique was employed to predict the shear strength of the columns. Significant conclusions are reached as follows.

- The ANN technique predicted the shear strength of rectangular hollow RC columns more accurately than that of existing formulas with R^2 value larger than 0.99.
- The width and height of cross-section (i.e., B and H) and the column height (L_v) were the most influential parameters on the calculated shear strength of the hollow columns.
- An effective GUI tool was developed and readily applied for predicting the shear strength and identifying failure modes of rectangular hollow RC columns in the design process and structural performance evaluation (https://github.com/duyduan1304/GUI_RCHollowColumn).

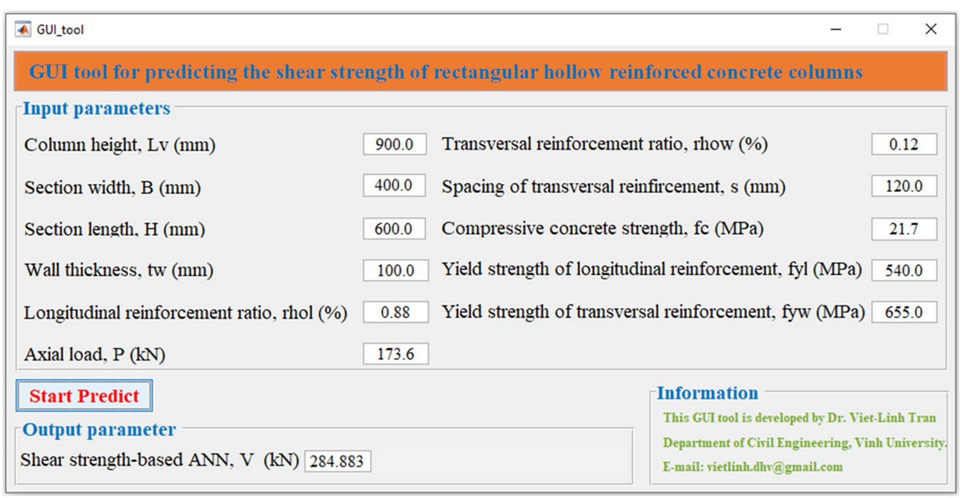

Fig. 6 GUI tool for predicting the strength of rectangular hollow RC columns

Detailed information of the database

ID	L_v(mm)	B(mm)	H(mm)	t_w(mm)	ρ_l(%)	ρ_w(%)	s(mm)	f_c'(MPa)	f_{yl}(MPa)	f_{yw}(MPa)	P(kN)	V (kN)	FM
1	1500	400	600	100	0.88	0.12	120	19	540	655	148	168	F
2	1500	600	400	100	0.88	0.12	120	21	540	655	166	117	F
3	900	400	600	100	0.88	0.12	120	22	540	655	174	278	FS
4	900	600	400	100	0.88	0.12	120	21	540	655	168	193	FS
5	900	450	450	75	1.07	0.13	75	35	550	550	236	217	FS
6	900	450	450	75	1.07	0.13	75	24	550	550	507	247	FS
7	900	450	450	75	1.07	0.13	75	32	550	550	763	297	FS
8	1350	450	450	75	1.79	0.25	75	30	550	550	239	217	FS
9	1350	450	450	75	1.79	0.25	75	30	550	550	501	209	FS
10	1350	450	450	75	1.79	0.25	75	33	550	550	515	226	FS
11	1350	450	450	75	1.79	0.25	75	31	550	550	762	258	FS
12	1400	450	450	75	1.79	0.20	75	20	625	390	245	190	FS
13	1400	450	450	75	1.79	0.09	75	28	435	437	251	130	FS
14	1400	450	450	75	1.79	0.09	75	29	560	443	257	170	S
15	1400	450	450	75	1.79	0.19	75	29	560	443	257	210	S
16	1400	450	900	75	1.79	0.20	75	20	625	390	249	240	S
17	1400	450	900	75	1.79	0.09	75	28	435	437	251	190	S
18	1400	450	900	75	1.79	0.09	75	29	560	443	257	190	S
19	1400	450	900	75	1.79	0.19	75	29	560	443	257	250	S
20	900	600	400	100	0.88	0.12	120	17	540	655	136	278	FS
21	900	400	600	100	0.88	0.12	120	17	540	655	136	193	FS
22	1800	500	500	120	0.19	0.11	50	58	476	480	975	333	F
23	1800	500	500	120	0.19	0.11	50	63	476	480	1471	360	F
24	1800	500	500	120	0.19	0.06	40	70	476	480	983	332	F
25	1800	500	500	120	1.88	0.52	40	61	476	363	1449	350	FS
26	1500	500	500	120	1.88	0.52	40	51	476	363	1013	364	S
27	1500	500	500	120	1.88	0.52	40	50	476	363	544	302	FS
28	5400	1500	1500	300	1.90	0.28	150	34	476	480	4355	2350	FS
29	5400	1500	1500	300	1.90	0.28	150	29	476	480	8800	2610	S
30	5400	500	500	120	1.90	0.03	150	33	476	480	553	2440	F
31	5400	500	500	120	1.90	0.03	150	31	476	480	982	2840	F
32	1800	500	500	120	1.90	0.11	50	33	476	480	499	271	F
33	1500	500	500	120	1.90	0.03	50	20	476	405	501	270	S
34	1500	500	500	120	1.90	0.03	50	27	423	405	500	298	F
35	1500	500	500	120	1.90	0.03	50	29	423	405	499	295	F
36	1500	500	500	120	1.90	0.03	50	27	406	405	498	278	F
37	1800	500	500	120	1.90	0.11	50	28	406	480	500	241	F
38	2000	550	550	140	1.33	0.09	100	48	617	405	4418	429	F
39	2000	550	550	140	1.33	0.09	100	57	617	405	2617	316	F
40	2000	550	550	110	1.58	0.09	100	60	617	405	5432	423	FS
41	6500	1500	1500	300	1.08	0.11	80	34	460	343	4015	1580	F
42	4500	1500	1500	300	1.08	0.04	120	34	460	510	4015	2420	F
43	3500	1500	1500	300	1.72	0.03	200	32	418	420	3686	2650	S
44	4500	1000	1000	250	1.53	0.17	80	22	376	343	1650	671	F
45	4500	1000	1000	250	1.53	0.17	80	47	408	406	2468	727	F
46	900	600	900	130	1.80	0.01	900	25	340	340	0	525	FS
47	1200	600	900	130	1.80	0.01	1200	25	340	340	0	445	FS

ID	L_v(mm)	B(mm)	H(mm)	t_w(mm)	ρ_l(%)	ρ_w(%)	s(mm)	f_c'(MPa)	f_{yl}(MPa)	f_{yw}(MPa)	P(kN)	V (kN)	FM
48	1500	600	900	130	1.80	0.01	1500	25	340	340	0	341	FS
49	1800	600	900	130	1.80	0.00	1800	25	340	340	0	259	FS
50	900	600	900	80	2.70	0.01	900	25	340	340	0	337	S
51	900	600	900	180	1.80	0.01	900	25	340	340	0	522	FS
52	900	600	900	160	1.07	0.01	900	18	300	300	0	458	FS
53	900	600	900	130	1.26	0.01	900	18	300	300	0	392	FS
54	1200	600	900	130	1.26	0.01	1200	18	300	300	0	334	FS
55	1500	600	900	130	1.26	0.01	1500	18	300	300	0	269	FS
56	1800	600	900	130	1.26	0.00	1800	18	300	300	0	203	FS
57	900	600	900	130	0.63	0.01	900	18	300	300	0	381	FS
58	3500	1500	1500	300	1.69	0.03	200	32	418	420	3594	2633	S
59	3500	1500	1500	300	1.69	0.03	200	18	420	413	3888	2544	F
60	3500	1500	1500	300	1.69	0.03	200	38	418	420	3621	1530	S
61	2000	500	500	200	1.13	0.25	40	30	460	400	1350	178	S
62	2000	500	500	200	1.13	0.25	40	30	460	400	675	171	F
63	2000	500	500	200	1.13	0.13	80	25	460	400	675	173	F
64	2000	500	500	200	1.13	0.25	40	50	460	400	1350	215	F
65	2000	500	500	200	1.13	0.25	40	50	460	400	675	177	F
66	2000	500	500	200	1.13	0.13	80	36	460	400	675	173	F
67	1440	360	500	120	1.40	0.35	40	41	300	300	1001	147	F
68	1440	360	500	120	2.10	0.35	40	41	300	300	1001	146	F
69	1440	360	500	120	1.40	0.35	40	41	300	300	2002	223	F
70	1440	360	500	120	2.10	0.35	40	41	300	300	2002	225	F
71	1440	360	500	120	1.40	0.35	40	41	300	300	615	207	FS
72	1440	360	500	120	2.10	0.35	40	41	300	300	615	261	FS
73	2880	360	500	120	1.40	0.35	40	41	300	300	615	70	F
74	2880	360	500	120	2.10	0.35	40	41	300	300	615	72	F
75	2880	360	500	120	1.40	0.35	40	41	300	300	1229	106	F
76	2880	360	500	120	2.10	0.35	40	41	300	300	1229	197	F
77	2880	360	500	120	2.10	0.25	55	41	300	300	615	69	F
78	3600	360	500	120	1.40	0.35	40	41	300	300	615	93	F
79	3600	360	500	120	2.10	0.35	40	41	300	300	615	95	F
80	3600	360	500	120	1.40	0.35	40	41	300	300	1229	110	F
81	3600	360	500	120	2.10	0.35	40	41	300	300	1229	123	F
82	3600	360	500	120	2.10	0.25	55	41	300	300	615	93	F
83	3025	750	750	120	2.84	0.06	60	31	335	320	937	282	F
84	3025	750	750	120	2.84	0.13	30	31	335	320	4687	496	FS
85	3025	750	750	120	2.84	0.09	40	28	335	320	2540	415	FS
86	3025	750	750	120	2.84	0.06	60	28	335	320	2540	418	FS
87	5750	1020	2740	170	0.40	0.09	120	35	500	500	3663	1300	F
88	13,250	1020	2740	170	0.70	0.09	120	35	500	500	3663	800	F
89	4200	730	975	150	6.41	0.27	40	57	393	390	1880	1124	F
90	4200	730	975	150	6.41	0.27	40	49	393	390	430	1084	F
91	1420	500	360	100	1.40	0.04	150	39	335	235	510	105	F
92	4500	1000	1000	250	1.53	0.17	80	47	408	406	2468	727	F
93	4500	1000	1000	250	1.38	0.17	80	47	408	406	2468	699	F
94	4500	1000	1000	250	1.38	0.11	120	47	408	406	2468	697	F
95	1200	320	320	85	1.57	0.34	50	34	295	345	0	70	S
96	1200	320	320	85	1.57	0.17	50	34	295	345	299	90	F
97	1200	320	320	85	1.57	0.34	50	34	295	345	299	85	F

ID	L_v(mm)	B(mm)	H(mm)	t_w(mm)	ρ_l(%)	ρ_w(%)	s(mm)	f_c'(MPa)	f_{yl}(MPa)	f_{yw}(MPa)	P(kN)	V (kN)	FM
98	650	320	320	85	1.57	0.17	50	34	295	345	299	175	S
99	650	320	320	85	1.57	0.34	50	34	295	345	299	190	S
100	4000	890	1000	70	0.98	0.26	50	39	437	374	1921	212	FS
101	4500	1000	1000	250	1.53	0.17	80	23	376	343	1710	671	FS
102	4500	1000	1000	250	1.38	0.17	80	23	376	343	1710	647	FS
103	1800	400	250	80	2.65	0.06	110	45	270	335	527	77	F
104	1800	400	250	80	2.65	0.06	110	45	270	335	702	82	F
105	1800	400	250	80	2.65	0.06	110	45	270	335	1054	84	F
106	1800	400	250	80	2.65	0.06	110	38	270	335	601	82	F
107	1350	400	400	100	2.53	0.07	100	24	374	363	230	200	FS
108	3780	840	840	150	1.15	0.16	60	59	390	343	1650	490	F
109	3780	840	840	150	1.15	0.08	120	40	390	343	1650	490	F
110	2100	840	840	150	1.15	0.16	60	45	390	343	1633	800	FS
111	2100	840	840	150	1.15	0.08	120	45	390	343	1633	800	FS
112	3780	840	840	150	1.15	0.16	60	40	390	343	1650	490	F
113	3780	840	840	150	1.15	0.16	60	50	357	343	1650	780	FS
114	2100	840	840	150	3.07	0.16	60	50	357	343	1633	1350	FS
115	1240	500	360	100	0.91	1.60	60	64	335	235	840	96	F
116	1240	500	360	100	1.33	1.60	60	64	335	235	840	186	F
117	1440	500	360	120	1.40	0.14	40	41	393	389	615	195	F
118	1440	500	360	120	1.40	0.14	40	41	393	389	1229	294	F
119	3500	1500	1500	300	1.08	0.03	200	33	423	392	3756	2600	S
120	8400	800	1600	160	1.15	0.03	200	51	500	700	1700	530	F

Author contributions X-BN: formal analysis, validation, visualization, writing—original draft. V-LT: conceptualization, software, writing—original draft. H-TP: visualization, validation. D-DN: methodology, formal analysis, validation; writing —original draft, writing—review & editing, supervision.

Data availability https://github.com/duyduan1304/GUI_RCHollowColumn.

Declarations

Conflicts of interest The authors declare that they have no conflicts of interest.

References

ACI-318–14 (2014). Building code requirements for structural concrete (ACI 318–14) and commentary. American Concrete Institute.

ASCE/SEI-41-06. (2007). *Seismic rehabilitation of existing buildings (ASCE/SEI 41–06)*. American Society of Civil Engineers, Reston, VA.

Ascheim, M., & Moehle, J. (1992). Shear strength and deformability of RC bridge columns subjected to inelastic cyclic displacements.

Asteris, P.G., & Mokos, V.G. (2019). Concrete compressive strength using artificial neural networks. *Neural Computing and Applications*, *32*(15), 11807–11826.

Biskinis, D. E., Roupakias, G. K., & Fardis, M. N. (2004). Degradation of shear strength of reinforced concrete members with inelastic cyclic displacements. *Structural Journal, 101*, 773–783.

Caglar, N., Pala, M., Elmas, M., & Eryılmaz, D. M. (2009). A new approach to determine the base shear of steel frame structures. *Journal of Constructional Steel Research, 65*, 188–195.

Calvi, G. M., Pavese, A., Rasulo, A., & Bolognini, D. (2005). Experimental and numerical studies on the seismic response of RC hollow bridge piers. *Bulletin of Earthquake Engineering, 3*, 267–297.

Cassese, P. (2017). Seismic performance of existing hollow reinforced concrete bridge columns. (Ph. D. Dissertation. Department of Structures for Engineering and …).

Cassese, P., De Risi, M. T., & Verderame, G. M. (2019). A modelling approach for existing shear-critical RC bridge piers with hollow rectangular cross section under lateral loads. *Bulletin of Earthquake Engineering, 17*, 237–270.

Cassese, P., De Risi, M. T., & Verderame, G. M. (2020). Seismic assessment of existing hollow circular reinforced concrete bridge piers. *Journal of Earthquake Engineering, 24*, 1566–1601.

Cheng, C.-T., Mo, Y., & Yeh, Y.-K. (2005). Evaluation of as-built, retrofitted, and repaired shear-critical hollow bridge columns under earthquake-type loading. *Journal of Bridge Engineering, 10*, 520–529.

EN-1998-1. (2004). Eurocode 8: Design of structures for earthquake resistance—Part 1: General rules. Seismic actions and rules for buildings.

Falcone, R., Lima, C., & Martinelli, E. (2020). Soft computing techniques in structural and earthquake engineering: A literature review. *Engineering Structures, 207*, 110269.

Farfani, H. A., Behnamfar, F., & Fathollahi, A. (2015). Dynamic analysis of soil-structure interaction using the neural networks and the support vector machines. *Expert Systems with Applications, 42*, 8971–8981.

Faria, R., Pouca, N. V., & Delgado, R. (2004). Simulation of the cyclic behaviour of R/C rectangular hollow section bridge piers via a detailed numerical model. *Journal of Earthquake Engineering, 8*, 725–748.

Feng, D.-C., Liu, Z.-T., Wang, X.-D., Jiang, Z.-M., & Liang, S.-X. (2020). Failure mode classification and bearing capacity prediction for reinforced concrete columns based on ensemble machine learning algorithm. *Advanced Engineering Informatics, 45*, 101126.

Gharehbaghi, S., Yazdani, H., & Khatibinia, M. (2019). Estimating inelastic seismic response of reinforced concrete frame structures using a wavelet support vector machine and an artificial neural network. *Neural Computing and Applications*, *32*, 2975–2988.

Ghee, A. B., Priestley, M. N., & Paulay, T. (1989). Seismic shear strength of circular reinforced concrete columns. *Structural Journal, 86*, 45–59.

Han, Q., Du, X., Zhou, Y., & Lee, G. C. (2013). Experimental study of hollow rectangular bridge column performance under vertical and cyclically bilateral loads. *Earthquake Engineering and Engineering Vibration, 12*, 433–445.

Kaveh, A., Dadras Eslamlou, A., Javadi, S., & Geran Malek, N. (2021). Machine learning regression approaches for predicting the ultimate buckling load of variable-stiffness composite cylinders. *Acta Mechanica, 232*, 921–931.

Kaveh, A., Eskandari, A., and Movasat, M. (2023). Buckling resistance prediction of high-strength steel columns using metaheuristic-trained artificial neural networks. (Elsevier), pp. 104853.

Kaveh, A., and Khavaninzadeh, N. (2023). Efficient training of two ANNs using four meta-heuristic algorithms for predicting the FRP strength. (Elsevier), pp. 256–272.

Kim, T.-H. (2019). Analytical seismic performance assessment of hollow reinforced-concrete bridge columns. *Magazine of Concrete Research, 71*, 719–733.

Kim, T.-H., Kim, I.-H., Lee, J.-H., & Shin, H. M. (2019). Hollow bridge columns with triangular confining reinforcement. *Canadian Journal of Civil Engineering, 46*, 467–480.

Kim, T.-H., Lee, J.-H., & Shin, H.-M. (2014a). Hollow reinforced concrete bridge column systems with reinforcement details for material quantity reduction: I. Development and verification. *Journal of the Earthquake Engineering Society of Korea, 18*, 1–8.

Kim, T.-H., Lee, J.-H., & Shin, H. M. (2014b). Performance assessment of hollow RC bridge columns with triangular reinforcement details. *Magazine of Concrete Research, 66*, 809–824.

Kowalsky, M. J., & Priestley, M. N. (2000). Improved analytical model for shear strength of circular reinforced concrete columns in seismic regions. *Structural Journal, 97*, 388–396.

Ma, Y., & Gong, J.-X. (2018). Probability identification of seismic failure modes of reinforced concrete columns based on experimental observations. *Journal of Earthquake Engineering, 22*, 1881–1899.

Mai, S. H., Tran, V.-L., Nguyen, D.-D., Nguyen, V. T., & Thai, D.-K. (2022). Patch loading resistance prediction of steel plate girders using a deep artificial neural network and an interior-point algorith. *Steel and Composite Structures, 45*, 159.

Mangalathu, S., Hwang, S.-H., & Jeon, J.-S. (2020). Failure mode and effects analysis of RC members based on machine-learning-based SHapley Additive exPlanations (SHAP) approach. *Engineering Structures, 219*, 110927.

Mangalathu, S., & Jeon, J.-S. (2019). Machine learning–based failure mode recognition of circular reinforced concrete bridge columns: Comparative study. *Journal of Structural Engineering, 145*, 04019104.

Mo, Y., Jeng, C.-H., & Perng, S. (2001). Seismic shear behavior of rectangular hollow bridge columns. *Structural Engineering and Mechanics, 12*, 429–448.

Mo, Y., & Nien, I. (2002). Seismic performance of hollow high-strength concrete bridge columns. *Journal of Bridge Engineering, 7*, 338–349.

Mo, Y., Wong, D., & Maekawa, K. (2003). Seismic performance of hollow bridge columns. *Structural Journal, 100*, 337–348.

Morfidis, K., & Kostinakis, K. (2018). Approaches to the rapid seismic damage prediction of r/c buildings using artificial neural networks. *Engineering Structures, 165*, 120–141.

Nguyen, D.-D., Tran, V.-L., Ha, D.-H., Nguyen, V.-Q., & Lee, T.-H. (2021a). *A machine learning-based formulation for predicting shear capacity of squat flanged RC walls* (pp. 1734–1747). Elsevier.

Nguyen, T.-H., Tran, N.-L., & Nguyen, D.-D. (2021b). Prediction of axial compression capacity of cold-formed steel oval hollow section columns using ANN and ANFIS Models. *International Journal of Steel Structures*. https://doi.org/10.1007/s13296-021-00557-z

Pekelnicky, R., Engineers, S., Chris Poland, S., & Engineers, N. (2012). ASCE 41–13: Seismic evaluation and retrofit rehabilitation of existing buildings. In: *Proceedings of the SEAOC*.

Phan, V.-T., Tran, V.-L., Nguyen, V.-Q., & Nguyen, D.-D. (2022). Machine learning models for predicting shear strength and identifying failure modes of rectangular RC columns. *Buildings, 12*, 1493.

Pinto, A., Molina, J., & Tsionis, G. (2003). Cyclic tests on large-scale models of existing bridge piers with rectangular hollow cross-section. *Earthquake Engineering & Structural Dynamics, 32*, 1995–2012.

Priestley, M. N., Verma, R., & Xiao, Y. (1994). Seismic shear strength of reinforced concrete columns. *Journal of Structural Engineering, 120*, 2310–2329.

Qi, Y.-L., Han, X.-L., & Ji, J. (2013). Failure mode classification of reinforced concrete column using Fisher method. *Journal of Central South University, 20*, 2863–2869.

Razzaghi, M. S., Safarkhanlou, M., Mosleh, A., & Hosseini, P. (2018). Fragility assessment of RC bridges using numerical analysis and artificial neural networks. *Earthquakes and Structures, 15*, 431–441.

Sezen, H., & Moehle, J. P. (2004). Shear strength model for lightly reinforced concrete columns. *Journal of Structural Engineering, 130*, 1692–1703.

Shin, M., Choi, Y. Y., Sun, C.-H., & Kim, I.-H. (2013). Shear strength model for reinforced concrete rectangular hollow columns. *Engineering Structures, 56*, 958–969.

Sun, Z., Wang, D., Wang, T., Wu, S., & Guo, X. (2019). Investigation on seismic behavior of bridge piers with thin-walled rectangular hollow section using quasi-static cyclic tests. *Engineering Structures, 200*, 109708.

Tran, N.-L., Nguyen, D.-D., & Nguyen, T.-H. (2022). Prediction of speed limit of cars moving on corroded steel girder bridges using artificial neural networks. *Sādhanā, 47*, 1–14.

Tran, V.-L., Thai, D.-K., & Nguyen, D.-D. (2020). Practical artificial neural network tool for predicting the axial compression capacity of circular concrete-filled steel tube columns with ultra-high-strength concrete. *Thin-Walled Structures, 151*, 106720.

Yang, C., Xie, L., & Li, A. (2019). Full-scale experimental and numerical investigations on seismic performance of square RC frame columns with hollow sections. *Journal of Earthquake Engineering*, *26*(1), 427–448.

Yeh, Y.-K., Mo, Y., & Yang, C. (2002a). Full-scale tests on rectangular hollow bridge piers. *Materials and Structures, 35*, 117–125.

Yeh, Y.-K., Mo, Y. L., & Yang, C. (2002b). Seismic performance of rectangular hollow bridge columns. *Journal of Structural Engineering, 128*, 60–68.

Zhu, L., Elwood, K., & Haukaas, T. (2007). Classification and seismic safety evaluation of existing reinforced concrete columns. *Journal of Structural Engineering, 133*, 1316–1330.

Publisher's Note Springer Nature remains neutral with regard to jurisdictional claims in published maps and institutional affiliations.